MT 26 International Conference on Magnet Technology
Vancouver, Canada | 2019

Level 2 Posters 1 Tue-Mo-Po2.06-03 [34] 08:45-10:45 24/09/2019

An optimized design approach for 14T actively shielded MRI magnets

Kaihong Wu, Yu Wu, Yi Shi, Aihua Xu, Qiangwang Hao, Chao Dai, Yuanyuan Ma, Yongliang Zhang, M. T. Hussain and Junrong Wu

1 - Institute of Plasma Physics, Chinese Academy of Sciences, PO Box 1126, Hefei, Anhui 230031, China
2 - University of Science and Technology of China,No.96,JinZhai Road Baohe District, Hefei, Anhui 230026, China

1. Introduction

In this paper, an optimized method to design superconducting magnets for 14T actively shielded MRI is proposed. At first, the feasible current-carrying region assumed as possible coil zone is subdivided into two-dimensional array grids, in which each grid represents one loop of a current-carrying conductor. Then the current distribution is obtained using linear programming by a detailed consideration of the superconductor consumption, central field strength, imaging region homogeneity and stray field leakage range. Afterwards the initial rectangular section of the magnet is determined by reshaping the current-carrying region and then the method of non-linear programming is adopted to refine the final configuration of each coil with the limitation of each coil position and section size. In addition, the spherical harmonics elimination of central magnetic fields is proposed as the optimization strategies used in the non-linear programming method to get the least level of inhomogeneity over the imaging region. Besides all the current centers are chosen based on the location of actual superconducting wires of each conductor. Finally this design method has obtained high field homogeneity in the central zone by four sets of coils with total length around 3.5m and inner diameter nearly 1m. The detailed analysis and optimization approach will be presented.

2. Optimization method

2.1 Linear Programming

The two-dimensional array source grids shown in Fig. 1 are the candidate domain for the main and shielded coils in which each grid represents one current loop of the actual conductor coaxial with the z-axis. The basic structure of the conductor shown in Fig. 2 is comprising of Nb_3Sn Rutherford cable (each strand shown as a yellow circle) and cooper stabilizer channel (orange):

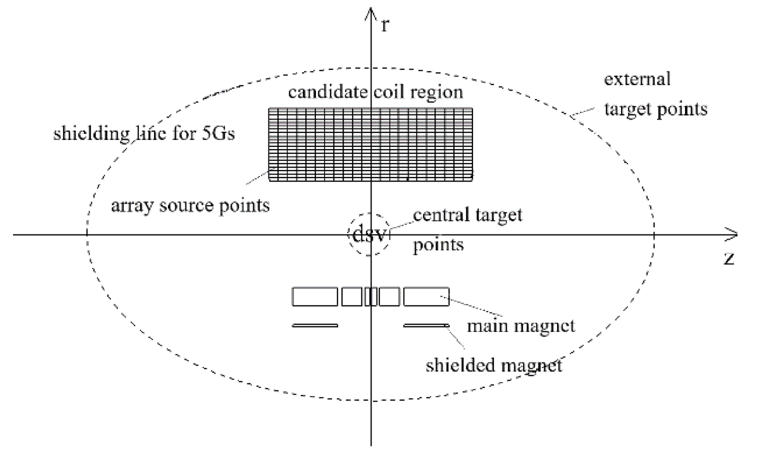

Fig. 1. Space arrangement of magnets, DSV and 5Gs stray field.

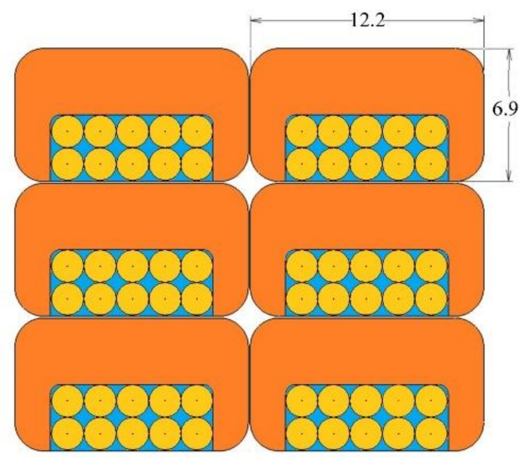

Fig. 2. Structure of Nb3Sn Rutherford cable-in-channel (RIC) conductor.

The magnetic field contribution of the *j-th* conductor current to the *i-th* central or external target point is: $B_{ij} = b_{ij} I_j$. In this way, the magnetic field equation for the target points on the DSV edge and shielding line can be established as:

$$\begin{aligned} B_{zdsv} &= A_{mk} \cdot I \\ B_{zstray} &= B_{nk} \cdot I \\ B_{rstray} &= C_{nk} \cdot I \end{aligned} \tag{1}$$

The formulation of linear programming can be obtained as follows: Where *F* is the objective function to describe by minimizing the volume of the superconductors. r_j and I_j denote radius and current of the *j-th* coil. *J* denotes the setting of current density in a superconductor. B_0 is the desired magnetic field strength, ε refers to the homogeneity factor, and I_{max} is the maximum current for one conductor.

$$Min \quad F = \frac{2\pi}{J} \sum_{j=1}^{k} r_j |I_j|$$

$$\begin{aligned} &\text{Subject to:} \\ &A_{mk} I \le B_0(1+\varepsilon) \\ &-A_{mk} I \le -B_0(1-\varepsilon) \\ &|B_{nk} I| \le B_{zstray} \\ &|C_{nk} I| \le B_{rstray} \\ &|I| \le I_{max} \end{aligned} \tag{2}$$

The initial configuration of the current region after LP is shown in Fig. 3. (a). The red region represents the main magnet with a positive current, blue represents the shielded magnet with a negative current, while most of the areas with no current are green. Since the region with current is irregular, reshaping and repositioning process is necessary. And after every adjustment, the settings of LP should be redefined to get the final rectangular section of the magnet shown in Fig. 3. (b). It is obviously seen that the axial edge of the shield magnet shall not exceed the end of the main magnet for the convenience of engineering installation and fixation.

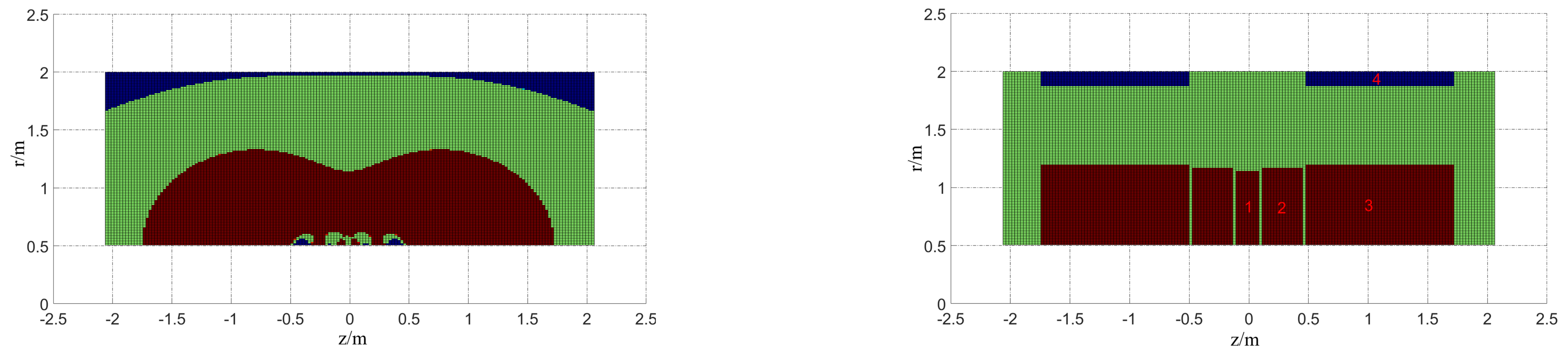

(a) (b)

Fig. 3. Current distribution of Linear Programming (a) initial configuration (b) after adjustment.

The main purpose of LP is to provide initial magnet configuration as shown in Fig. 3. (b) for the subsequent non-linear optimization. The better the initial value is, the faster the convergence rate of the non-linear optimization will be.

2.2 Non-Linear Programming

The axial component of the central magnetic field at a point *(r, θ)* derived from one current-carrying circular coil coaxial with the z-axis is given by:

$$B_z = \frac{\mu_0 I}{2r} \sum_{n=0}^{\infty} sin\theta' P_{n+1}^1(cos\theta') \cdot \left(\frac{r}{a}\right)^{n+1} P_n(cos\theta) \qquad r < a \tag{3}$$

Where a, θ' denote the radius and azimuth angle of the circular current. If the coaxial coils are configured symmetrically along the mid-plane with equal current, all odd terms of B_z will be eliminated but all even terms will duplicate because:

$$P_{n+1}^1(cos\theta) = (-1)^{n+2} P_{n+1}^1\big(cos(\pi - \theta)\big) \tag{4}$$

Then the remaining terms are as follows: The term n=0 represents the constant term of the magnetic field B_0 which should be reserved, and the other terms need to be eliminated as many as possible.

$$B_z = \mu_0 I sin\theta' P_{n+1}^1(cos\theta') a^{-(n+1)} \cdot r^n P_n(cos\theta) \qquad r < a, n = 0,2,4 \cdots \tag{5}$$

In this way, the sphere harmonics elimination strategy can be established, where W_n refers to the remaining source terms.

$$W_n = \sum_{j=1}^{K} \mu_0 I \sin\theta_j P_{n+1}^1(cos\theta_j)\left(\frac{1}{a_j}\right)^{n+1} \qquad r < a, n = 0,2,4 \cdots \tag{6}$$

K refers to the number of the current centers which is determined by the total number of actual superconducting strands of all the Rutherford cable in channel (RIC) conductors shown in Fig. 2. This method considers the detailed current-carrying locations which makes the MRI magnet design more feasible and accurate. At last the formulation of non-linear programming can be obtained as follows:

$$Min \quad Q = [(W_0 - B_0) + W_2 + W_4 + W_6 + W_8] \times 10^6$$

$$\begin{aligned} &\text{Subject to:} \\ &\sqrt{B_{zstray}^2 + B_{rstray}^2} - B_{shield} < 0 \\ &r_{min}(i) \le r_{inner}(i) \le r_{min}(i) + dr(i) && i = 1,2,3,4 \\ &r_{outer}(i) = r_{inner}(i) + Nr(i) \cdot tw && i = 1,2,3,4 \\ &z_{right}(i-1) \le z_{left}(i) && i = 2,3 \\ &z_{right}(i) = z_{left}(i) + Nz(i) \cdot nw && i = 1,2,3,4 \\ &z_{right}(4) \le z_{right}(3) \\ &0 \le z_{left}(1) \end{aligned} \tag{7}$$

Where Q is the objective function to describe by minimizing the central field inhomogeneity. *i* refers to the mark of magnet shown in Fig. 3. (b). Since the coil is symmetrical, only the right half part will be considered, and the coil region marked 1 denote the section of z≥0. B_{shield} is the limited value of the stray field, r_{inner} and r_{outer} denote the inner and outer radius, while z_{left} and z_{right} are the left and right axial positions of each coil. And r_{min} is the minimum inner radius for each coil, and *dr* is the allowable radial position adjustment. *Nr* and *tw* denote the number of conductor layers and the width of the conductor in the radial direction. *Nz* and nw represent the number of conductor turns and the length of the conductor in the axial direction. The shield coils share the same power supply with the main coils but carry current in the opposite direction.

4. Optimization Results

The homogeneity over the 45cm DSV region and the distribution of the stray field calculated from the final magnet structure are shown in Fig. 4. (a) and (b) respectively. As shown in these figures, after optimization of non-linear programing the inhomogeneity over the 45cm DSV has been reduced to around 1ppm and the 5 gauss line of the stray field are restricted to a cylinder with 10.5m radius and 11.5m half-length. All of these results can meet our design requirements.

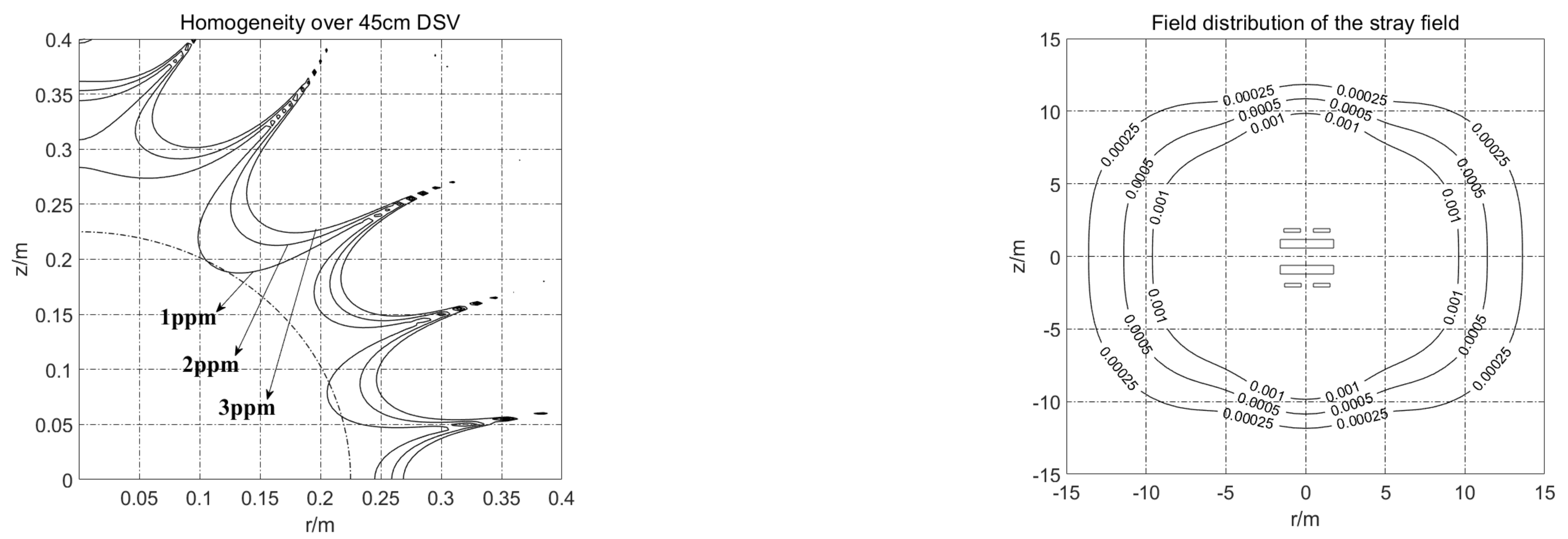

(a) (b)

Fig. 4. (a) Homogeneity for 45cm DSV (b) 5GS line of the stray field

Besides in order to vividly display the field homogeneity, Fig. 5. (a) and (b) give the results of field map over the central region and sphere surface with a 45cm diameter. The homogeneity over the imaging region is evidently seen in these figures with maximum and minimum field of 14.000002 T and 13.999986 T respectively. And from these results it can be noted that this optimization approach works quite well to design superconducting magnets with extensive homogeneous field distribution

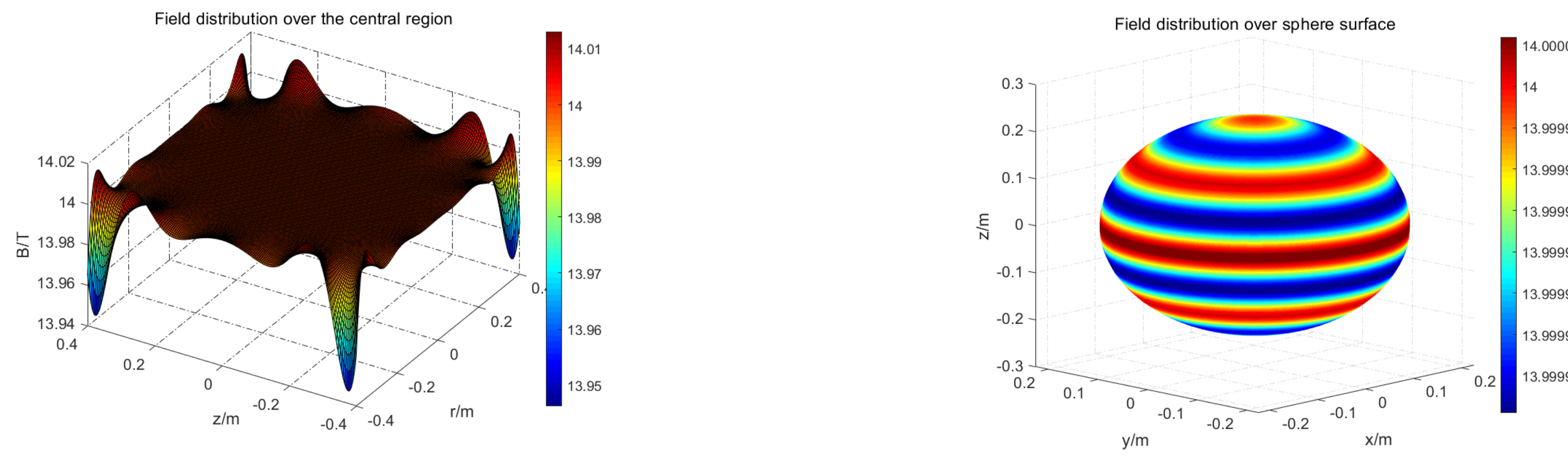

(a) (b)

Fig. 5. Field distribution (a) over the central region (b) over the sphere surface with a 45cm diameter

5. Conclusion

Linear and non-linear combined optimization approach are used in the design of the 14T actively shielded MRI superconducting magnets. The linear programming gives rise to the initial rectangular section of the magnet configuration and then the non-linear programming is adopted to refine the structure. Besides sphere harmonics elimination is applied as the optimization strategy with fast speed and good efficiency and the detailed superconducting wires considered as the actual current centers for calculation makes the overall design reliable. Finally this optimization method has obtained high field homogeneity over the central region and limited level of stray field with good performance, and these design approaches can also be used to design more superconducting magnets for real MRI applications